Computers in Biology and Medicine 135 (2021) 104593

Contents lists available at ScienceDirect

Computers in Biology and Medicine

journal homepage: www.elsevier.com/locate/compbiomed

An integrated framework for evaluation on typical ECG-derived respiration waveform extraction and respiration

Kejun Dong [a,b], Li Zhao [a,**], Zhipeng Cai [b], Yuwen Li [b], Jianqing Li [b], Chengyu Liu [b,*]

[a] School of Information Science and Engineering, Southeast University, Nanjing, 210096, PR China
[b] School of Instrument Science and Engineering, Southeast University, Nanjing, 210096, PR China

ARTICLE INFO

Keywords:
ECG-Derived respiration breathing rate waveform correlation a comprehensive and integrated evaluation

ABSTRACT

Objective: ECG-derived respiration (EDR) methods have been developed during the past decades to obtain respiration-relevant information. However, it is still necessary to compare the performance of these methods under uniform conditions for reasonable application. *Approach*: In this paper, the performance of 10 feature-based EDR methods was evaluated comprehensively on three aspects: sampling rate, noise, and window length. The Fantasia database was used in this study, as it contained ECG signals and simultaneously measured respiration signals. The performance was quantified by two parameters: waveform correlation and breathing rate (BR) errors. *Main results*: The BR errors of AM_{area}, AM_{QR}, AM_R were all below 2 beats per minute (bpm) when the sampling rate was above 150 Hz, while they decreased sharply by about 60% when the sampling rate was below 150 Hz. FM_{RR} presented stable performance with an error below 2 bpm at different sampling rates. The effect of noise was obviously found in amplitude-based EDR methods, with the maximum decreased by about 40% in waveform correlation. For all EDR methods, significant increase of BR errors occurred with the window shorting from 32 s to 16 s in the frequency-based technique. In addition, about 30%–40% of the window cannot obtain the BR error, calculated based on the time-based technique, within an 8 s window. *Significance*: We proposed a comprehensive and integrated evaluation on typical ECG-derived respiration waveform extraction and respiration rate calculation, providing references for algorithm selection based on different requirements.

1. Introduction

Respiration is one of the important vital signs, and its functional changes have been proven to be diagnostic indicators for different diseases [1]. The monitoring and analysis of respiration are a key means to detect sleep-relevant disorders (sleep apnea syndrome [2], obstructive sleep apnea [3] and mental health (stress, anxiety [4], depression, etc.). Currently, airflow sensors, impedance plethysmography [5] and inductance plethysmography are used for respiration recording, while they are too bulky for comfortable, long-term, dynamic respiration monitoring applications [6]. As the most measured vital signal, electrocardiogram (ECG) is modulated by respiration in both beat morphology and heart rate variability [1]. Therefore, most of the current researches focuses on ECG-derived respiration (EDR) waveforms and subsequent breathing rate (BR) calculation for clinical applications.

Although many EDR methods have been proposed based on features and filters during the past decades, the feature-based EDR methods have received more attention in recent years. The features used to derive respiration includes amplitude-relevant features (the area of QRS complex [1], R peak amplitude [7], slope-relevant features (the upslope of the QRS complex [8], the angle around R wave [9], frequency-relevant features (RR interval [10], QRS duration [11], etc.) and baseline wander-relevant features (mean value between consecutive troughs [7], mean amplitude of troughs and peaks, etc.). An amplitude-based EDR method (area of QRS complex) was proposed and tested in 2000 Computers in Cardiology Conference Challenge, the comparison result with plethysmogram signals (correlation coefficient 0.78) showed that the proposed method was effective in respiration extraction [12]. Ruangsuwana et al. [7] proposed and compared three feature-based EDR methods (amplitude-based, frequency-based, baseline wander-based), the results showed that the frequency-based method and baseline wander-based method were similar in effect, and were superior to the amplitude-based method. Lázaro et al. [9] proposed three slope-based EDR methods (slopes of the QRS complex, angle around R-peak), and

* Corresponding author.
** Corresponding author.
E-mail addresses: zhaoli@seu.edu.cn (L. Zhao), chengyu@seu.edu.cn (C. Liu).

https://doi.org/10.1016/j.compbiomed.2021.104593
Received 21 April 2021; Received in revised form 5 June 2021; Accepted 17 June 2021
Available online 23 June 2021

tested them in ECG signals under tilt and stress conditions. The BR error between the extracted respiration with simultaneously recorded respiration were 0.50 ± 4.11% and 0.52 ± 8.99% for the tile test and stress test, respectively. These feature-based EDR methods all can effectively obtain respiratory information from ECG signals. However, it is still necessary to compare the performance of these methods under uniform conditions for reasonable employment of methods.

In order to verify the performance and practicality of these methods in different applications, some studies have been conducted to compare these proposed feature-based EDR methods. Correa et al. [2] evaluated three feature-based EDR method (R peak amplitude, heart rate variability and R wave area) on the Apnea-ECG database, the comparison between the extracted respiration and three real respiratory signals (oronasal, chest and abdominal inductance plethysmography) showed that R wave area-based EDR method could extract more relevant respiration waveform (correlation coefficient 0.55). Boyle et al. [13] compared the respiration waveforms extracted by six EDR methods from ambulatory single-lead ECGs with simultaneously measured respiration waveforms by airflow sensor, and they found that RR interval-derived EDR method could be used for respiration extraction from dynamic single-lead ECG without significant differences from traditional methods. Widjaja et al. [14] investigated similarity between the respiration waveforms derived from ECGs and simultaneously recorded respiratory signal, the results showed that R amplitude-based method could generate the best respiratory signals (mean square error 0.63). Charlton et al. [5] assessed hundreds of algorithm combinations of estimating BR from ECG, which referred to more than ten EDR methods. The performance was compared with impedance pneumography through several statistical analysis of BR. The top ranked result was from RR interval-based, QR amplitude-based and baseline wander-based EDR methods with a bias of 0.0 breaths per minute (bpm). Ten EDR methods were used to extract respiration waveform from ECG signals, and the derived respiratory rates, wave morphology, and cardiorespiratory information were compared with reference respiratory signals. The results on three datasets (Fantasia, Sleep and Driver datasets) showed that QRS slope-based method outperformed the other methods under different conditions, and indicated that signal quality of ECGs had a crucial effect on the performance of EDR methods [4]. Although these studies have evaluated different EDR methods under different conditions, more work is still needed to study the effect of comprehensive conditions on the respiration extraction of EDR methods in order to achieve a uniform agreement for reasonable use of these methods.

In this study, an integrated framework for evaluation on typical EDR waveform extraction and respiration rate calculation was proposed, which included three aspects: the influence of sampling rate and signal-to-noise ratio (SNR) on the EDR waveform extraction, and the influence of window length on the BR calculation. Firstly, ten feature-based EDR methods were adopted to extract respiratory waveform from ECG signal. To evaluate the similarity between the extracted respiratory waveform and simultaneously measured respiration waveform essentially, the correlation was first compared. Then, BR calculated from the extracted respiratory waveform was compared with that from simultaneously measured respiration waveform furtherly. All the experiments were implemented on Fantasia Database.

2. Methods

2.1. Data

The Fantasia database [15] was used in our study, which contained 120-min ECG and respiration recordings around the thorax measured from 40 healthy subjects. The sampling rates of these physiological signals were all 250 Hz. In order to reduce the computational complexity, only a continuous first 10-min ECG and respiration signal of each recording were analyzed in this work.

2.2. Signal preprocessing and postprocessing

To remove the high-frequency components of raw ECG recording, a lowpass filter with 35 Hz cutoff frequency was used. Then, the Pan & Tompkins algorithm [16] was performed for R-peak detection. Thereafter, the respiration waveform was extracted from ECG and resampled at 5 Hz for additional noise elimination.

2.3. Respiration waveform extraction

After preprocessing, the respiration waveform was extracted from the filtered 10-min ECG signal. In this study, ten existing feature-based EDR methods were adopted for respiration waveform extraction and classified into four groups based on amplitude, slope, frequency, and baseline wander. The calculation of their corresponding features was shown in Fig. 1.

2.4. Amplitude-based methods (AM)

(1) AM_{area}: Sobron et al. [1] defined the closed area of QRS complexes from Q-peak to S-peak (as l in Fig. 1) as $Feature_1$ to reflect the effect of respiratory on ECG morphology.

$$Feature_1 = \int_{T_Q}^{T_S} V_{ECG}(t) - l(t)dt, \tag{1}$$

where T_Q is onset (Q-peak), T_S is offset (S-peak). V_{ECG} is the amplitude of preprocessed ECG and l is the line connecting Q-peak and S-peak.

(2) AM_{QR}: The amplitude variation between R-peak and Q-peak on ECG ($Feature_2$) was modified by Charlton et al. [5], according to the respiratory-induced amplitude variation proposed by Karlen et al. [17].

$$Feature_2 = V_R - V_Q, \tag{2}$$

where V_R and V_Q are the amplitudes of R-peak and Q-peak in a QRS complex.

(3) AM_R and AM_Q: It was reported that changes in ECG amplitude could reflect respiration Ruangsuwana et al. [7], therefore, the amplitudes of R-peak and Q-peak were extracted as $Feature_3$ and $Feature_4$ in this study. The detailed illustration of these features was shown in Fig. 1.

2.5. Slope-based methods (SM)

(1) SM_{angle}: $Feature_5$ was defined by Lázaro et al. [9] as the angle (θ_R in Fig. 1) between the maximal upslope (n_U in Fig. 1) and downslope (n_D in Fig. 1) around R-peak. The general angular expression is defined as follows:

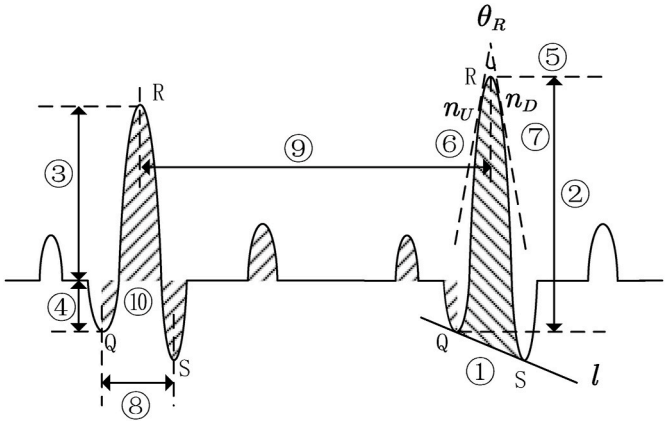

Fig. 1. Demonstrations of the features extracted from ECG for the recovery of respiration waveform. Label - indicate the features introduced in section 2.3.

$$\theta = \arctan\left(\left|\frac{n_U - n_D}{1 + n_U * n_D}\right|\right), \tag{3}$$

For the clinical purpose, the time axis and voltage axis should be rescaled to match the particular case of conventional ECG tracings, where a speed of 25 mm/s and a gain of 10 mm/mV were used as in Romero et al. [18], and formula (3) was changed to equation (4) accordingly:

$$Feature_5 = \theta_R = \arctan\left(\left|\frac{n_U - n_D}{0.4 * (6.25 + n_U * n_D}\right|\right), \tag{4}$$

(2) SM_{QR} and SM_{RS}: Apart from the angle formed by upslope (n_U) and downslope (n_D), the slopes themselves could also reflect respiration [8]. Therefore, n_U and n_D were also used in this study as $Feature_6$ and $Feature_7$.

2.6. Frequency-based methods (FM)

(1) FM_{QS}: The duration of the QRS complex, the time calculated from the onset to the offset of the QRS complex, was used as $Feature_8$ to demonstrate the frequency modulated feature of respiration on ECG [11].

$$Feature_8 = T_S - T_Q, \tag{5}$$

where T_S and T_Q are the time of offset and onset defined by the method in this section.

(2) FM_{RR}: Respiratory sinus arrhythmia (RSA) represented the respiration modulation on heart rate [10]. The variation of intervals between two consecutive R peaks was adopted as $Feature_9$:

$$Feature_9 = T_{R_{i+1}} - T_{R_i}, i = 1, 2, \ldots, \tag{6}$$

where $T_{R_{i+1}}$ and T_{R_i} are locations of two consecutive R peaks in the ith heartbeat.

2.7. Baseline wander-based methods (BM)

(1) BM_{QRS}: The area between two consecutive Q-peak was calculated as $Feature_{10}$ referring to the ECG area defined by Ruangsuwana et al. [7].

$$Feature_{10} = \frac{1}{Q_{i+1} - Q_i}\int_{Q_i}^{Q_{i+1}} V_{ECG}(t)dt, i = 1, 2, \ldots, \tag{7}$$

where Q_i is the location for the ith Q-peak.

2.8. Breathing rate calculation

After obtaining the respiration extracted from the feature-based EDR method proposed above, BR was computed on different window length as another aspect to evaluate the performance of existing methods. To avoid the disturbance caused by redundant frequency component in calculating BR, the extracted respiration waveforms were band-pass filtered (0.15–0.4 Hz) according to breathing rate range (9–24 bpm) [19]. In addition, in order to simultaneously consider the influence of frequency domain and time domain on BR calculation, the frequency-based and time-based BR estimation methods were adopted.

2.9. Frequency-based technique

Considering the improvement in frequency resolution, autoregressive modelling (AR) [20] with the order of 8 [10] was selected as the frequency-based BR calculation method in this study, rather than the traditional Fourier-based analysis. The details of AR were given as follows:

$$x(n) = -\sum_{k=1}^{p} a_k x(n-k) + e(n), \tag{8}$$

where $x(n)$ is the output at $t = n$, $x(n-k)$ is the output at $t = n-k$, a_k is the parameter linearly relating the previous values to current values and $e(n)$ is the error term.

To obtain the frequency domain components (poles) of power spectrum of respiratory signal, equation (8) was transformed to z domain as equation (9). Then, the phase angle (θ) of the pole nearest to the unit circle was selected as equation (10).

$$H(z) = \frac{1}{1 - \sum_{k=1}^{p}(1 - a_k z^{-k})}, \tag{9}$$

$$\theta = 2f\pi\Delta t, \tag{10}$$

where Δt is the sampling interval of the original time series.

2.10. Time-based technique

The modified Mason's algorithm [21] was adopted for its simple implementation and high robustness. It indicated the peaks and troughs were detected when the gradient changed from positive to negative and negative to positive respectively. Then, the peaks less than the mean and troughs greater than the means were eliminated [22]. In addition, the peaks (troughs) were eliminated if they were within 0.5 s of the previous peaks (troughs) [23]. And the respiratory rate was acquired from valid peaks and troughs.

To validate the two BR calculation methods before evaluating the performance of EDR methods, the errors of the calculated BR and the BR based on manually annotated respiratory peaks were compared. Fig. 2 shows the BR comparison result between two BR methods with manual annotation. The BR was both 16.7 bpm no matter from time-based technique and annotated reference (Fig. 2 (a)), as the detected peaks of respiratory waveform were consistent with the manually annotated ones. The BR error of the frequency-based technique and annotated reference was 1.5 bpm, indicating that the calculated BR was clinically relevant to the annotated BR as the error was within ± 2 bpm referring to van Loon et al. [24].

2.11. Effects of three factors on the performance of EDR methods

In order to evaluate the performances of the existing EDR methods, the effects of three different factors on the waveform correlation and BR errors were compared: sampling rate, SNR and window length. The overall evaluation procedure was illustrated in Fig. 3 and implemented based on the open-source toolbox accessible in Charlton et al. [5]. All the data processing and computations were executed on a regular PC using the MATLAB software framework, v. R2020a (Mathworks, Natick, MA, USA).

2.12. Sampling rate

Currently, there is no clear standard for the sampling rate of the ECG signal used to extract the respiratory waveform, and the sampling rate has an important impact on the storage resources and energy consumption of the acquisition device. Therefore, the original 250 Hz ECG signals from the Fantasia database were down-sampled to 200, 150, 100 and 50 Hz, and the effect of sampling rate on the performance of EDR methods was evaluated.

2.13. Signal to noise ratio

With the prevalence of wearable devices, ECG signals are vulnerable to noise pollution. Therefore, the influence of SNR on the EDR methods was considered in this study. For this reason, different levels of Gaussian

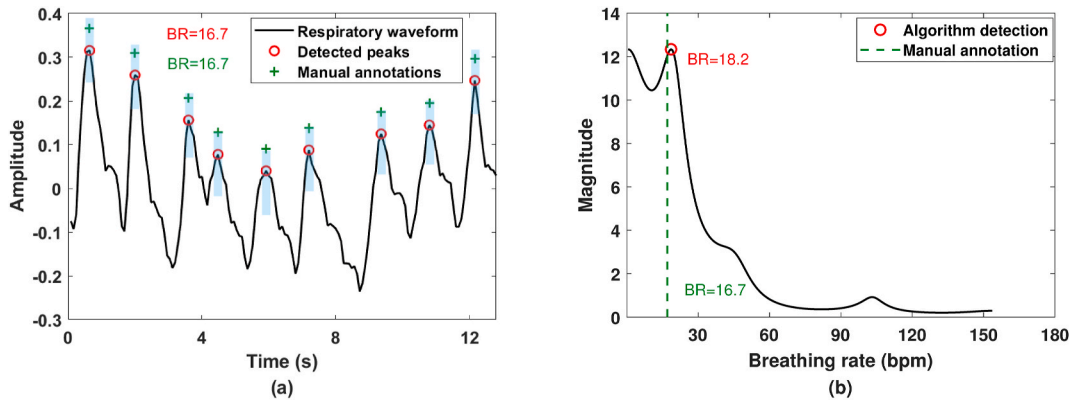

Fig. 2. The demonstration of verification results of (a) time-based BR calculation and (b) frequency-based BR calculation. In Fig. 2(a), the detected peak locations are marked as red circles, and the manual annotations are marked as green plus signs. In Fig. 2(b), the detected breathing rate is marked as the red circle, and the manual annotated breathing rate is located at the green dashed line.

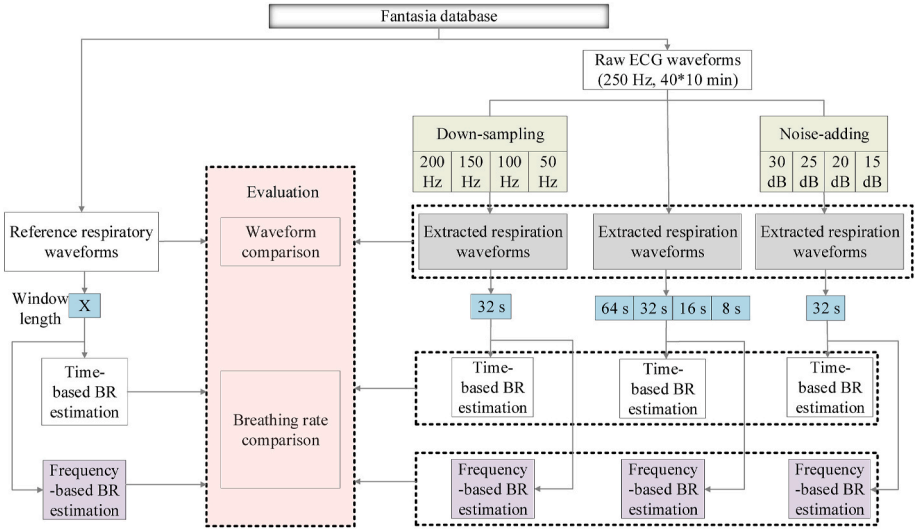

Fig. 3. The structure of evaluation process. The symbol X stands for corresponded window lengths in each scenario.

noise were added into 250 Hz raw ECG signal according to practice (30 dB was clean and 15 dB was polluted), and noisy ECG signals with SNRs of 30, 25, 20 and 15 dB were obtained.

2.14. Window length

The selection of appropriate window length for BR calculation is associated with the complexity and accuracy of EDR method. Then, four window lengths (64, 32, 16 and 8s) were adopted for BR calculation from extracted respiratory waveform, and their results were evaluated by two BR methods.

2.15. Evaluation methods

The performance of ten EDR methods on extracted respiratory waveform and calculated BR was quantified using waveform correlation and mean absolute error (MAE). Waveform correlation: To calculate the cross-correlation of the extracted respiratory waveform and the simultaneous measured respiratory signal, the 10-min extracted and measured respiratory waveform were divided into 32 s segment firstly. Then, the correlation coefficients of each segment were computed respectively, and the mean value of the absolute maximal correlation coefficient calculated from each 32 s segment was defined as the waveform correlation of the 10-min signal. MAE: The BR for extracted and measured respiratory waveform was obtained from both time- and frequency-based techniques described in section 2.4. Then, the absolute errors between the calculated BR and the reference BR were obtained according to different window length. The mean value of these absolute errors was computed as MAE of the 10-min signal. The definition of MAE was described as follows:

$$MAE(k) = \frac{1}{N}\sum_{k=1}^{N}\left|f_{EDR}(k) - f_{ref}(k)\right| \tag{11}$$

where $f_{EDR}(k)$ and $f_{ref}(k)$ are the BR of kth window length of EDR waveform and reference respiratory waveform, respectively.

3. Experiments and results

3.1. Evaluation results of extracted respiratory waveforms

To evaluate the performance of the ten EDR methods on respiratory waveform extraction, the cross-correlation between the extracted respiratory waveform and the simultaneous measured respiratory signal was calculated and compared (Fig. 4). The detailed comparison result was illustrated in Table 1. Fig. 4 (a) demonstrated the comparison results of ten EDR methods under different sampling rates. It can be seen that, as expected, the waveform correlation of almost all methods reduced as

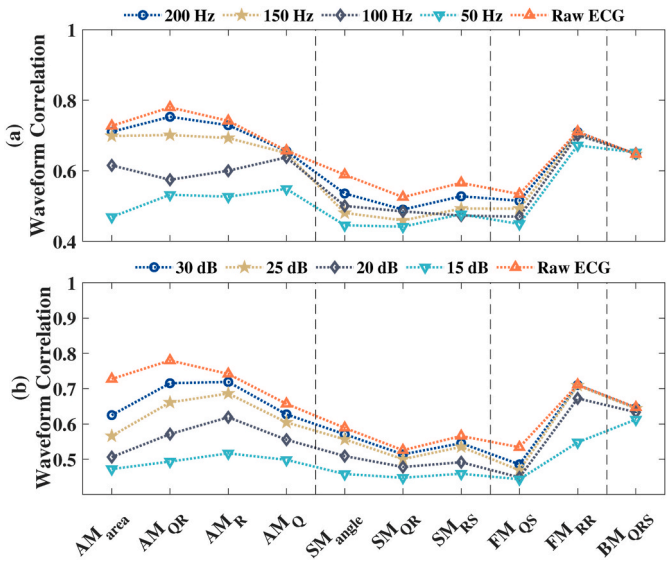

Fig. 4. The correlation of extracted respiratory and reference waveforms under (a) down-sampling and (b) noise adding. The EDR methods are referred to in section 2.3.

the sampling rate decreased, except for AM_{QRS}. This phenomenon was particularly obvious in amplitude-based EDR methods. In addition, AM_{QR} showed the best performance when the sampling rate was greater than 150 Hz, and the waveform correlation of FM_{RR} was the largest in the range of 150 Hz–50 Hz. The effects of SNR on the performance of ten EDR methods was shown in Fig. 4 (b). Similar to the effect of sampling rate, the increase in noise added to the raw ECG would reduce the waveform correlation of most methods. However, the performance of MB_{QRS} was almost unaffected by SNR, which could exhibit stable waveform correlation under different noise levels.

Table 2 illustrated the relative errors of waveform correlation under down-sampling/noise adding. It could be seen that the waveform correlation of AM_{area} decreased slightly at 200 Hz and 150 Hz, and dropped sharply below 150 Hz (relative error −36%). However, the relative error of BM_{QRS} at different sampling rate were all 0%, indicating that it was suitable for applications with stable performance requirements. For waveform correlation under noise adding, almost all the relative errors of amplitude-based EDR methods were less than −30% at 15 dB, which meant that noise had a great influence on these methods. On the contrary, the waveform correlation of BM_{QRS} only decreased to −6% at 15 dB, which proved the robustness of this method.

3.2. Evaluation results of breathing rates

3.2.1. The effects of sampling rate

Fig. 5 illustrated the MAEs of BR between reference and estimations, calculated from time-based method (a) and frequency-based (b) method, respectively. It could be seen that the MAEs of AM_{area}, AM_{QR} and AM_R were within the ± 2 bpm limitation at the sampling rate larger than 150 Hz. FM_{RR} was the most stable one, and its MAEs were within the ± 2 bpm limitation at all sampling rates. For frequency-domain BR estimation (Fig. 5 (b)), the MAEs of these methods were all larger than 2 bpm, and all these methods presented a similar performance at each sampling rate. The detailed MAEs were demonstrated in Table 3 (see Table 4).

The relative errors of the MAEs under down-sampling and the original MAEs were shown in Table 4. It was obvious that the variations of relative errors calculated from amplitude-based EDR methods were more remarkable than other methods both for time-based BR estimation and frequency-based BR estimation. Especially, the MAEs of AM_{QR} and AM_R increased almost two times from 200 Hz to 50 Hz in the time-based estimation, which was 126% and 119%, respectively.

3.2.2. The effects of noise

Fig. 6 showed the MAE of proposed EDR methods with the SNR decreasing from 30 dB to 15 dB (see Table 4). In time-based BR estimation, the MAEs of AM_{area}, AM_{QR} and AM_R were below 2 bpm when the SNR is higher than 20 dB. The MAEs of FM_{RR} almost remained

Table 1
Waveform correlations between extracted respiratory and reference waveforms from all EDR methods under down-sampling and noise adding.

Sampling rate/SNR	AM				SM			FM		BM
	AM_{area}	AM_{QR}	AM_R	AM_Q	SM_{angle}	SM_{QR}	SM_{RS}	FM_{QS}	FM_{RR}	BM_{QRS}
raw	0.73	**0.78**	0.74	0.66	0.59	0.53	0.57	0.53	0.71	0.65
200 Hz	0.71	**0.75**	0.73	0.66	0.54	0.49	0.53	0.52	0.71	0.65
150 Hz	0.7	0.7	0.69	0.65	0.48	0.46	0.49	0.49	**0.71**	0.65
100 Hz	0.62	0.57	0.6	0.64	0.5	0.48	0.47	0.47	**0.7**	0.65
50 Hz	0.47	0.53	0.53	0.55	0.45	0.44	0.48	0.45	**0.67**	0.65
raw	0.73	**0.78**	0.74	0.66	0.59	0.53	0.57	0.53	0.71	0.65
30 dB	0.62	**0.72**	**0.72**	0.63	0.57	0.51	0.55	0.49	0.71	0.64
25 dB	0.57	0.66	0.69	0.6	0.56	0.5	0.53	0.47	**0.71**	0.64
20 dB	0.51	0.57	0.62	0.56	0.51	0.48	0.49	0.45	**0.67**	0.63
15 dB	0.47	0.49	0.52	0.5	0.46	0.45	0.46	0.44	0.55	**0.61**

Table 2
Relative errors between waveform correlation under down-sampling/noise adding and the original waveform correlation.

Down-sampling/Noise adding	AM				SM			FM		BM
	AM_{area} (%)	AM_{QR} (%)	AM_R (%)	AM_Q (%)	SM_{angle} (%)	SM_{QR} (%)	SM_{RS} (%)	FM_{QS} (%)	FM_{RR} (%)	BM_{QRS} (%)
$\Delta_{raw\to 200\ Hz}$	−3	−4	−1	**0**	−8	−8	−7	−2	**0**	**0**
$\Delta_{raw\to 150\ Hz}$	−4	−10	−7	−2	−19	−13	−14	−8	**0**	**0**
$\Delta_{raw\to 100\ Hz}$	−15	−27	−19	−3	−15	−9	−18	−11	−1	**0**
$\Delta_{raw\to 50\ Hz}$	−36	−32	−28	−17	−24	−17	−16	−15	−6	**0**
$\Delta_{raw\to 30dB}$	−15	−8	−3	−5	−3	−4	−4	−8	**0**	−2
$\Delta_{raw\to 25dB}$	−22	−15	−7	−9	−5	−6	−7	−11	**0**	−2
$\Delta_{raw\to 20dB}$	−30	−27	−16	−15	−14	−9	−14	−15	−6	**−3**
$\Delta_{raw\to 15dB}$	−36	−37	−30	−24	−22	−15	−19	−17	−23	**−6**

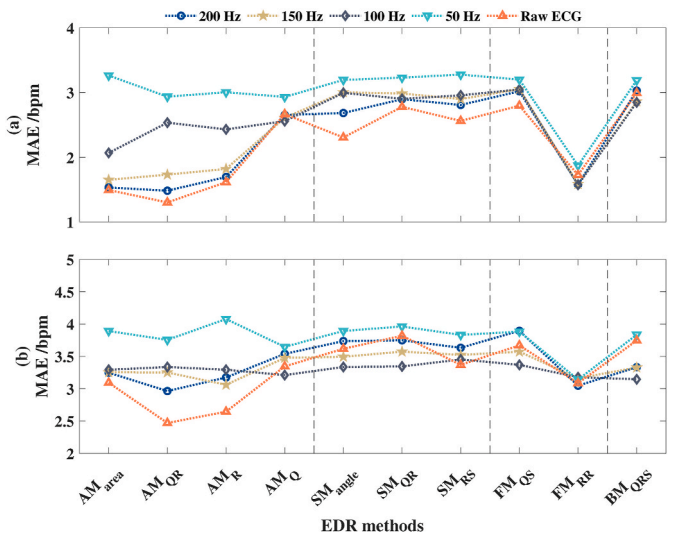

Fig. 5. Mean absolute error based on (a) time-domain BR estimation and (b) frequency-domain BR estimation. The EDR methods are referred to in section 2.3. Five lines in each subfigure represent results obtained from ECG signals with a specific sampling rate: grey-raw ECG, blue-200 Hz, orange-150 Hz, purple-100 Hz, green-50 Hz.

unchanged at the SNR is higher than 15 dB, and they were all below 2 bpm. Although BM_{QRS} supplied the most stable performance at different SNRs, the MAEs were all out of the ± 2 bpm limitation. In addition, the MAEs of these methods were all above 2.5 bpm when estimated by frequency-based technique. The detailed MAEs were demonstrated in Table 5.

The relative errors of the noise-added MAEs and the original MAEs were shown in Table 6. For most methods, the relative errors varied slightly in frequency-based BR estimation compared to those in time-based BR estimation. Typically, the MAEs of AM_{area} and AM_{QR} increased by more than 100% from 30 dB to 15 dB.

3.2.3. *The effects of window length*

Fig. 7 illustrated the MAEs of BR between reference and estimations calculated from different window length by time-based method (a) and frequency-based (b) method, respectively. In Fig. 7 (a), the MAE increased gradually in time-domain BR estimation as the window length declined from 64 s to 16 s. From all the results, only MAEs of most amplitude-based EDR methods were within the ± 2 bpm limitation with all adopted window length. Due to a large number of invalid windows, the result of the 8 s window was not drawn. In Fig. 7 (b), there was an obvious gap between the MAEs from 32 s window length and 16 s window length, and the MAEs calculated from each EDR method, under the window length around the upper and lower boundary of the gap, were almost unchanged. The detailed MAEs were demonstrated in Table 7 (see Table 8).

Table 8 showed the relative errors with the window length decreasing from 64 s to 8 s. Almost all the relative errors increased at least 20% when the window length decreased from 32 s to 16 s from both time-based technique and frequency-based technique. However, the relative errors varied greatly in time-based BR estimation compared to in frequency-based BR estimation.

Fig. 8 showed the proportion of windows failing to estimate BR for each EDR method under 8 s window length. For most EDR methods, it was found that about 30%–40% of the 8 s window could not find enough peaks to calculate BR based on time-based technique. Especially, the proportion of invalid windows reached about 50% in AM_Q and BM_{QRS}. Therefore, the remaining results obtained from the valid window could not reveal the performance of each method in the 8 s window.

4. Discussion

The contribution of this article is to provide objective clarification

Table 3
MAEs of BR between reference and estimations under down-sampling.

Sampling rate	AM				SM			FM		BM
	AM_{area}	AM_{QR}	AM_R	AM_Q	SM_{angle}	SM_{QR}	SM_{RS}	FM_{QS}	FM_{RR}	BM_{QRS}
					Time-based MAE (bpm)					
raw	1.49	**1.3**	1.61	2.66	2.3	2.78	2.56	2.8	1.72	2.99
200 Hz	1.53	**1.48**	1.69	2.65	2.68	2.9	2.81	3.02	1.58	3.03
150 Hz	1.65	1.73	1.82	2.61	3	2.98	2.9	3.05	**1.58**	2.86
100 Hz	2.07	2.53	2.43	2.56	3	2.9	2.96	3.05	**1.57**	2.85
50 Hz	3.26	2.94	3	2.93	3.2	3.23	3.28	3.2	**1.87**	3.19
					Frequency-based MAE (bpm)					
raw	3.09	**2.47**	2.64	3.35	3.62	3.82	3.37	3.67	3.08	3.75
200 Hz	3.25	**2.96**	3.17	3.54	3.74	3.75	3.63	3.89	3.05	3.33
150 Hz	3.25	3.25	3.06	3.48	3.49	3.57	3.52	3.57	**3.16**	3.33
100 Hz	3.29	3.33	3.29	3.21	3.34	3.34	3.45	3.37	3.18	**3.15**
50 Hz	3.89	3.75	4.08	3.65	3.89	3.96	3.83	3.88	**3.14**	3.83

Table 4
Relative errors of the MAEs under down-sampling and the original MAEs.

Down-sampling	AM				SM			FM		BM
	AM_{area}	AM_{QR}	AM_R	AM_Q	SM_{angle}	SM_{QR}	SM_{RS}	FM_{QS}	FM_{RR}	BM_{QRS}
Time-based relative errors (%)										
$\Delta_{raw\to 200\ Hz}$	3	14	5	**0**	17	4	10	8	−8	1
$\Delta_{raw\to 150\ Hz}$	11	33	13	**−2**	30	7	13	9	−8	−4
$\Delta_{raw\to 100\ Hz}$	39	95	51	**−4**	30	**4**	16	9	−9	−5
$\Delta_{raw\to 50\ Hz}$	119	126	86	10	39	16	28	14	9	**7**
Frequency-based relative errors (%)										
$\Delta_{raw\to 200\ Hz}$	5	20	20	6	3	−2	8	6	**−1**	−11
$\Delta_{raw\to 150\ Hz}$	5	32	16	4	−4	−7	4	**−3**	**3**	−11
$\Delta_{raw\to 100\ Hz}$	6	35	25	−4	−8	−13	**2**	−8	3	−16
$\Delta_{raw\to 50\ Hz}$	26	52	55	9	7	4	14	6	**2**	**2**

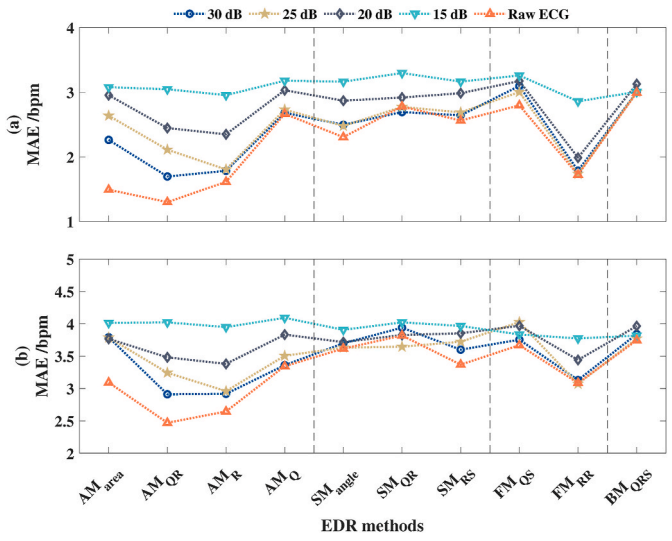

Fig. 6. Mean absolute error based on (a) time-domain BR estimation and (b) frequency-domain BR estimation. The EDR methods are referred to in section 2.3. Five lines in each subfigure represent results obtained from ECG signals with a certain SNR: grey-raw ECG, blue-30 dB, orange-25 dB, purple-20 dB, green-15 dB.

about the performance of typical EDR methods under practical issues. Due to the effectiveness of published EDR algorithms is a concern for many researchers and the performance agreement has been hardly achieved from current publications, the evaluation of these methods could provide other researchers the reference for employing them.

The ECG is a standard tool for cardiovascular disease diagnosis, while it is recorded by medical staff at different sampling rate based on their experience. Whether the sampling rate of the ECG signal will affect the extraction of the respiratory waveform needs in-depth research. O'Brien and Heneghan [25] evaluated the effect of 200 Hz sampling rate on the performance of three amplitude-relevant and baseline wander-relevant methods, and they found that the respiratory waveforms extracted from these methods at this sampling rate were correlated with simultaneously measured respiratory signal (correlation coefficient 0.75). The influence of 250 Hz sampling rate on two amplitude- and frequency-based EDR methods were analyzed [26]. The

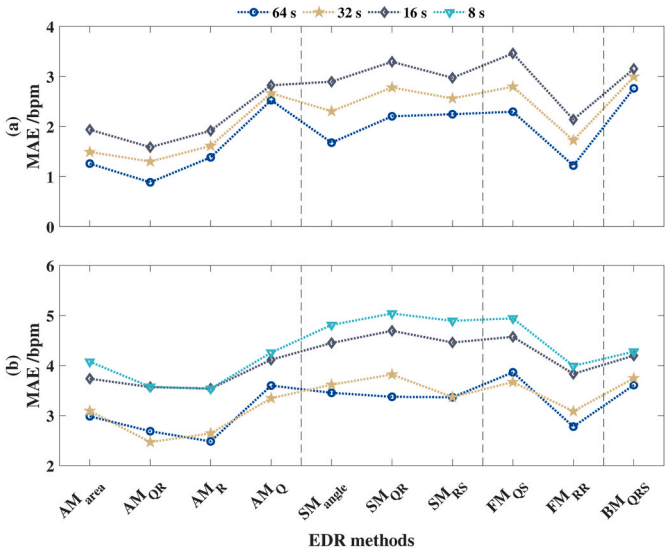

Fig. 7. Mean absolute error based on (a) time-domain BR estimation and (b) frequency-domain BR estimation. The EDR methods are referred to in section 2.3. Lines in each subfigure represent results estimated within a certain window length: blue-64 s, orange-32 s, purple-16 s, green-8 s.

Table 5
MAEs of BR between reference and estimations under noise adding.

SNR	AM				SM			FM		BM
	AMarea	AMQR	AM_R	AM_Q	SM_{angle}	SM_{QR}	SM_{RS}	FM_{QS}	FM_{RR}	BM_{QRS}
Time-based MAE (bpm)										
raw	1.49	**1.3**	1.61	2.66	2.3	2.78	2.56	2.8	1.72	2.99
30 dB	2.26	**1.7**	1.78	2.68	2.5	2.69	2.64	3.1	1.79	3
25 dB	2.64	2.11	1.81	2.73	2.48	2.77	2.69	3	**1.74**	3
20 dB	2.95	2.45	2.35	3.03	2.87	2.92	2.98	3.17	**1.99**	3.13
15 dB	3.08	3.04	2.95	3.18	3.16	3.3	3.16	3.26	**2.86**	3
Frequency-based MAE (bpm)										
raw	3.09	**2.47**	2.64	3.35	3.62	3.82	3.37	3.67	3.08	3.75
30 dB	3.79	**2.91**	2.92	3.36	3.7	3.94	3.6	3.75	3.13	3.84
25 dB	3.79	3.24	**2.96**	3.51	3.63	3.65	3.72	4.03	3.07	3.77
20 dB	3.77	3.48	**3.38**	3.83	3.72	3.83	3.85	3.97	3.44	3.96
15 dB	4.01	4.02	3.95	4.09	3.91	4.02	3.97	3.83	**3.77**	3.82

Table 6
Relative errors of the MAEs under noise adding and the original MAEs.

Noise adding	AM				SM			FM		BM
	AM_{area}	AM_{QR}	AM_R	AM_Q	SM_{angle}	SM_{QR}	SM_{RS}	FM_{QS}	FM_{RR}	BM_{QRS}
Time-based relative errors (%)										
$\Delta_{raw\to 30dB}$	52	31	11	1	9	−3	3	11	4	**0**
$\Delta_{raw\to 25dB}$	77	62	12	3	8	**0**	5	7	1	**0**
$\Delta_{raw\to 20dB}$	98	88	46	14	25	**5**	16	13	16	**5**
$\Delta_{raw\to 15dB}$	107	134	83	20	37	19	23	16	66	**0**
Frequency-based relative errors (%)										
$\Delta_{raw\to 30dB}$	23	18	11	**0**	2	3	7	2	2	2
$\Delta_{raw\to 25dB}$	23	31	12	5	**0**	−4	10	10	0	1
$\Delta_{raw\to 20dB}$	22	41	28	14	3	**0**	14	8	12	6
$\Delta_{raw\to 15dB}$	30	63	50	22	8	5	18	4	22	**2**

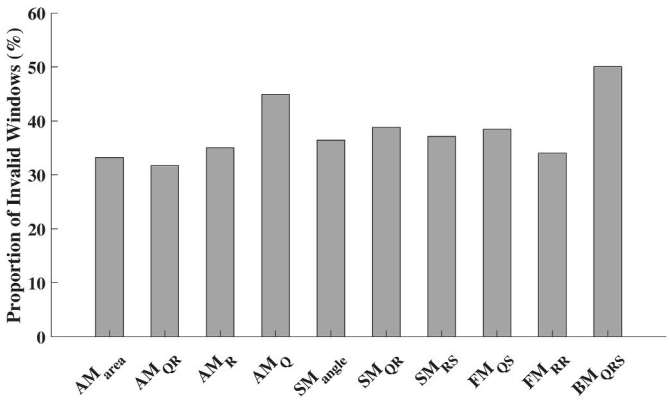

Fig. 8. Proportion of 8 s windows failing to estimate BR in time domain.

waveform correlation between the R-wave amplitude-based method extracted respiratory waveform and the airflow sensor recorded respiratory waveform reached 0.73, which was consistent with our method (waveform correlation 0.74 at 250 Hz). In addition, the breathing error was used as another parameter to evaluate the effect of 300 Hz sampling rate on the performance of three EDR methods (amplitude-, frequency- and baseline wander-based) besides respiratory waveform correlation [7]. These studies investigated the effect of specific sampling rates on the performance of several EDR methods, which was part of our work. Charlton et al. [27] evaluated several filter- and feature-based EDR methods with the sampling rate ranging from 500 Hz to 50 Hz. Their findings indicated the correlation between EDR signals and the reference oral-nasal pressure signals was higher as the sampling rate was higher (not up to 250 Hz). Our study could be considered as a continuation and extension of their work based on following points: firstly, the evaluation of sampling rate was investigated on a different but widely used and publicly available database, to realize the verification of consistent findings on other datasets. Secondly, the evaluated EDR methods were classified into four classes based on amplitude, frequency, slope and baseline wander. The performance of EDR methods among different classes was furtherly explored in our study. Therefore, the significant effects of sampling rate on amplitude-based EDR methods were found. Oppositely, the baseline wander-based method provided a relatively stable performance.

The detection accuracy of ECG signal peak is sensitive to noise, and ECG signal is susceptible to noise pollution, especially under wearable conditions. Therefore, the effect of noise on the performance of ten EDR methods was evaluated on three databases with different noise level [4]. They found that most EDR methods were sensitive to noise, especially for methods of kernel principal component analysis [14], principal component analysis [28] and R-wave amplitude [7]. However, this evaluation provided the non-specific effect of noise on EDR methods since the noise level was based on the sources of data. In our study, white Gaussian noise was added to ECG data to quantify the SNR with different values and the performance of specific noise level was evaluated. The similar result was also observed that the waveform correlation of the R-wave amplitude (AM_R)-based method decreased by 30% with SNR declined to 15 dB. The reason is obvious that the peaks used in amplitude-based methods are vulnerable to noise, while frequency-based methods focus on limited bandwidth and the remaining methods depend on the comprehensive result of data around the peaks. To compare the effects of noise level on performances of several BR estimation methods, Adami et al. [29] added noise to generate signals with SNR of 0 dB, 5 dB, 10 dB, 20 dB, 40 dB, which realized the performance evaluation through BR errors in both low and high noise situations. However, the extracted respiratory waveform morphology was not attracted attention in their evaluation, which was valuable for evaluating the performance of EDR methods and provided the guarantee for reliable BR estimation. Therefore, our study realized the performance evaluation in essence. In our study, prior to BR calculation, the waveform correlation between EDR signals and reference signals was as a primary parameter to evaluate effects of noisy data with the SNR of 15 dB–30 dB. Moreover, the consistent step of 5 dB in the smaller SNR range resulted in a high resolution of the performance variation, which could capture the exact and detailed performance information caused by noise.

For quasi real-time and mobile applications, the window length

Table 7
MAEs of BR between reference and estimations under window length shorting.

Window length	AM				SM			FM		BM
	AM_{area}	AM_{QR}	AM_R	AM_Q	SM_{angle}	SM_{QR}	SM_{RS}	FM_{QS}	FM_{RR}	BM_{QRS}
Time-based MAE (bpm)										
64 s	1.26	**0.88**	1.38	2.53	1.68	2.2	2.24	2.3	1.22	2.76
32 s	1.49	**1.3**	1.61	2.66	2.3	2.78	2.56	2.8	1.72	2.99
16 s	1.94	**1.59**	1.92	2.82	2.9	3.29	2.97	3.46	2.14	3.15
8 s	–	–	–	–	–	–	–	–	–	
Frequency-based MAE (bpm)										
64 s	2.98	2.69	**2.48**	3.6	3.45	3.37	3.37	3.86	2.78	3.61
32 s	3.09	**2.47**	2.64	3.35	3.62	3.82	3.37	3.67	3.08	3.75
16 s	3.74	3.57	**3.54**	4.11	4.45	4.69	4.46	4.57	3.83	4.2
8 s	4.08	3.57	**3.54**	4.26	4.81	5.04	4.89	4.94	3.99	4.28

Table 8
Relative errors of the MAEs under window length shorting and the original MAEs.

Window shorting	AM				SM			FM		BM
	AM_{area}	AM_{QR}	AM_R	AM_Q	SM_{angle}	SM_{QR}	SM_{RS}	FM_{QS}	FM_{RR}	BM_{QRS}
Time-based relative errors (%)										
$\Delta_{64\ s\to32\ s}$	18	48	17	**5**	37	26	14	22	41	8
$\Delta_{64\ s\to16\ s}$	54	81	39	**11**	73	50	33	50	75	14
$\Delta_{64\ s\to8\ s}$	–	–	–	–	–	–	–	–	–	–
Frequency-based relative errors (%)										
$\Delta_{64\ s\to32\ s}$	4	−8	6	−7	5	13	**0**	−5	11	4
$\Delta_{64\ s\to16\ s}$	26	33	43	**14**	29	39	32	18	38	16
$\Delta_{64\ s\to8\ s}$	37	33	43	**18**	39	50	45	28	44	19

related algorithm complexity needs to be considered. Major evaluations on effects of window length focus on the duration between 16 s and 300 s [17,30–32]. Some researchers [30,33,34], tested the influence of 32 s and 64 s window length on the MAEs of calculated BR on the CapnoBase and BIDMC datasets, and they observed that the MAE decreased with the increase of the window length. Charlton [35] carried out the experiment on the RRest-healthy dataset to optimize more than ten BR estimations for different window length (25 s, 32 s, and 50 s) of the respiratory signal. The findings indicated a lager duration provided the limited improvement in performance. Moreover, Karlen et al. [17] investigated the effect of three window length (64 s, 32 s and 16 s) on the performance of BR estimation from the photoplethysmogram, they also observed a positive trend for a lower error rate in larger windows, which was similar to our observation in BR estimation from ECG. However, little attention has been paid in furtherly shorted window length, which is of importance on evaluating the performance and option of appropriate window length for time-based BR techniques. Therefore, the 8 s window length was also evaluated in this paper. It is worth noting that for most EDR methods, about 30%–40% of the window cannot obtain the BR result, calculated based on the time-domain technique, within an 8 s window. The reason lies in the difficulty to find enough peaks for BR calculation in such a short window.

Apart from the typical feature-based EDR methods, filter-based and machine learning methods are other categories for respiration extraction. Orphanidou [36] proposed a filter-based EDR method which employed ensemble empirical mode decomposition to identify respiratory mode from ambulatory ECG. The validation of this technique with respiratory Impedance pneumography showed a mean error of 1.8 bpm and a relative error of 10.3%. However, the mode mixture may occur with empirical mode decomposition applied, which meant respiratory component could be distributed in multiple intrinsic mode functions resulting in the uncertainty of extracted respiratory signal. In Ref. [5], the comparison between both feature- and filter-based methods was made and the top performances for respiration extraction were all given from feature-based techniques. Compared to conventional methods, few studies on EDR algorithms are based on feature-learning algorithms as far. Ravichandran et al. [37] introduced a deep learning network for extracting the respiratory signal from PPG and compared it with two conventional amplitude- and frequency-based EDR methods. The similarity and reported errors of extracted respiration from proposed network were found to be better. Whereas, results of machine learning algorithms depend highly on the training datasets, which means different training datasets would give inconsistent results. In addition, the performance of this kind of learning algorithms is decided by the size of training data, which certainly increases computation complexity for more accurate results. Oppositely, the feature-based EDR methods we evaluated are obviously simpler, which requires low computation complexity. Therefore, these methods could be realized on the low power platform, especially appropriate for wearable devices.

5. Conclusion

An integration framework of performance evaluation was carried out systematically to investigate the effects of sampling rate, noise level and window length on performance of EDR methods and BR calculations. The evaluated EDR methods were classified into 4 groups: amplitude-based, frequency-based, slope-based and baseline wander-based. The effects of sampling rate and noise on amplitude-based EDR methods were more significant in contrast to other groups. Besides, the performance of BR was estimated and compared by time-based and frequency-based methods. It was found that the calculated MAEs from the time-based technique were less than those from the frequency-based technique, which was consistent with the result of Charlton et al. [5]. The reason may be that the respiratory signal for the time-based technique is not required to be quasi-stationary.

Some limitations should be mentioned in this study. Currently, the performance is only evaluated on the Fantasia database, which is clean and recorded under a static environment. The performances of EDR methods on the noisy and dynamic data need to be evaluated in future work. Another limitation is that BR calculation is based on basic peak detection. The accuracy is affected by the detected peaks. Therefore, a more automatic and accurate BR detector is necessary. In addition, although these EDR methods perform well in a static environment, more efforts should be devoted to developing new methods to extract respiration waveform from ECG accurately in a dynamic environment.

In this study, the performance of 10 feature-based ECG-derived respiration methods was quantified, based on three aspects: sampling rate, SNR and window length, by waveform correlation and breathing rate calculation. The results showed that the AM_{QR} could be applied to occasions with high accuracy requirements, and FM_{RR} performed better in stability applications. In conclusion, these findings were meaningful for providing references for algorithm selection based on different requirements.

Acknowledge

This work was supported by the National Key Research and Development Program of China (2019YFE0113800), the Natural Science Foundation of Jiangsu Province (BK20190014 and BK20192004), the National Natural Science Foundation of China (81871444, 62001105, 62001111 and 62071241), the Aviation Science Foundation Project (20200029069001), the Fundamental Research Funds for the Central Universities (2242021R20045).

References

[1] A. Sobron, I. Romero, T. Lopetegi, Evaluation of methods for estimation of respiratory frequency from the ECG, Comput. Cardiol. 37 (2010) 513–516.
[2] L.S. Correa, E. Laciar, A. Torres, R. Jané, Performance evaluation of three methods for respiratory signal estimation from the electrocardiogram, in: Proc. 30th Annu. Int. Conf. IEEE Eng. Med. Biol. Soc. EMBS'08 - "Personalized Healthc. Through Technol., IEEE, 2008, pp. 4760–4763.
[3] J. Harrington, P.J. Schramm, C.R. Davies, T.L. Lee-Chiong, An electrocardiogram-based analysis evaluating sleep quality in patients with obstructive sleep apnea, Sleep Breath. 17 (2013) 1071–1078.
[4] C. Varon, J. Morales, J. Lázaro, M. Orini, M. Deviaene, S. Kontaxis, D. Testelmans, B. Buyse, P. Borzée, L. Sörnmo, P. Laguna, E. Gil, R. Bailón, A comparative study of ECG-derived respiration in ambulatory monitoring using the single-lead ECG, Sci. Rep. 10 (2020), 5704–5704.
[5] P.H. Charlton, T. Bonnici, L. Tarassenko, D.A. Clifton, R. Beale, P.J. Watkinson, An assessment of algorithms to estimate respiratory rate from the electrocardiogram and photoplethysmogram, Physiol. Meas. 37 (2016) 610–626.
[6] R. Bailon, L. Sörnmo, P. Laguna, ECG-derived respiratory frequency estimation, Adv. Methods Tools ECG Data Anal. 1 (2006) 215–243.
[7] R. Ruangsuwana, G. Velikic, M. Bocko, Methods to extract respiration information from ECG signals. ICASSP, IEEE Int. Conf. Acoust. Speech Signal Process., IEEE, 2010, pp. 570–573.
[8] E. Pueyo, L. Sörnmo, P. Laguna, QRS slopes for detection and characterization of myocardial ischemia, IEEE Trans. Biomed. Eng. 55 (2008) 468–477.
[9] J. Lázaro, E. Gil, R. Bailón, A. Mincholé, P. Laguna, Deriving respiration from photoplethysmographic pulse width. Med. Biol. Eng. Comput., IEEE, 2013, pp. 233–242.
[10] C. Orphanidou, S. Fleming, S.A. Shah, L. Tarassenko, Data fusion for estimating respiratory rate from a single-lead ECG, Biomed. Signal Process Contr. 8 (2013) 98–105.
[11] K. Ramya, K. Rajkumar, Respiration rate diagnosis using single lead ECG in real Time, Global J. Med. Res. 13 (2013) 7–12.
[12] P. de Chazal, T. Penzel, C. Heneghan, Automated detection of obstructive sleep apnoea at different time scales using the electrocardiogram, Physiol. Meas. 25 (2004) 967–983.
[13] J. Boyle, N. Bidargaddi, A. Sarela, M. Karunanithi, Automatic detection of respiration rate from ambulatory single-lead ECG, IEEE Trans. Inf. Technol. Biomed. 13 (2009) 890–896.
[14] D. Widjaja, C. Varon, A. Dorado, J.A. Suykens, S. Van Huffel, Application of kernel principal component analysis for single-lead-ecg-derived respiration, IEEE Trans. Biomed. Eng. 59 (2012) 1169–1176.
[15] N. Iyengar, C.K. Peng, R. Morin, A.L. Goldberger, L.A. Lipsitz, Age-related alterations in the fractal scaling of cardiac interbeat interval dynamics, Am. J. Physiol. Regul. Integr. Comp. Physiol. 271 (1996) R1078–R1084.
[16] J. Pan, W.J. Tompkins, A real-time QRS detection algorithm, IEEE Trans. Biomed. Eng. 32 (1985) 230–236.

[17] W. Karlen, S. Raman, J.M. Ansermino, G.A. Dumont, Multiparameter respiratory rate estimation from the photoplethysmogram, IEEE Trans. Biomed. Eng. 60 (2013) 1946–1953.
[18] D. Romero, M. Ringborn, P. Laguna, E. Pueyo, Detection and quantification of acute myocardial ischemia by morphologic evaluation of QRS changes by an angle-based method, J. Electrocardiol. 46 (2013) 204–214.
[19] D.S. Quintana, M. Elstad, T. Kaufmann, C.L. Brandt, B. Haatveit, M. Haram, M. Nerhus, L.T. Westlye, O.A. Andreassen, Resting-state high-frequency heart rate variability is related to respiratory frequency in individuals with severe mental illness but not healthy controls, Sci. Rep. 6 (2016) 1–8.
[20] S. Fleming, L. Tarassenko, M. Thompson, D. Mant, Non-invasive measurement of respiratory rate in children using the photoplethysmogram, in: Proc. 30th Annu. Int. Conf. IEEE Eng. Med. Biol. Soc. EMBS'08 - "Personalized Healthc. Through Technol, IEEE, 2008, pp. 1886–1889.
[21] S. Fleming, Measurement and Fusion of Non-invasive Vital Signs for Routine Triage of Acute Paediatric Illness, Ph.D. Thesis, Oxford University, 2010.
[22] A. Johansson, Neural network for photoplethysmographic respiratory rate monitoring, Med. Biol. Eng. Comput. 41 (2003) 242–248.
[23] B. Mazzanti, C. Lamberti, J. De Bie, Validation of an ECG-derived respiration monitoring method, Comput. Cardiol. 30 (2003) 613–616.
[24] K. van Loon, L.M. Peelen, E.C. van de Vlasakker, C.J. Kalkman, L. van Wolfswinkel, B. van Zaane, Accuracy of remote continuous respiratory rate monitoring technologies intended for low care clinical settings: a prospective observational study, Can. J. Anesth. 65 (2018) 1324–1332.
[25] C. O'Brien, C. Heneghan, A comparison of algorithms for estimation of a respiratory signal from the surface electrocardiogram, Comput. Biol. Med. 37 (2007) 305–314.
[26] D. Cysarz, R. Zerm, H. Bettermann, M. Frühwirth, M. Moser, M. Kröz, Comparison of respiratory rates derived from heart rate variability, ECG amplitude, and nasal/oral airflow, Ann. Biomed. Eng. 36 (2008) 2085–2094.
[27] P.H. Charlton, T. Bonnici, L. Tarassenko, J. Alastruey, D.A. Clifton, R. Beale, P. J. Watkinson, Extraction of respiratory signals from the electrocardiogram and photoplethysmogram: technical and physiological determinants, Physiol. Meas. 38 (2017) 669–690.
[28] P. Langley, E.J. Bowers, A. Murray, Principal component analysis as a tool for analyzing beat-to-beat changes in ECG features: application to ECG-derived respiration, IEEE Trans. Biomed. Eng. 57 (2009) 821–829.
[29] A. Adami, R. Boostani, F. Marzbanrad, P.H. Charlton, A new framework to estimate breathing rate from electrocardiogram, photoplethysmogram, and blood pressure signals, IEEE Access 9 (2021) 45832–45844.
[30] S.G. Fleming, L. Tarassenko, A Comparison of signal processing techniques for the extraction of breathing rate from the photoplethysmogram, Int. J. Biol. Life Sci. 2 (2006) 233–237.
[31] A. Garde, W. Karlen, J.M. Ansermino, G.A. Dumont, Estimating respiratory and heart rates from the correntropy spectral density of the photoplethysmogram, PloS One 9 (2014), e86427.
[32] M.A. Pimentel, A.E. Johnson, P.H. Charlton, D. Birrenkott, P.J. Watkinson, L. Tarassenko, D.A. Clifton, Toward a robust estimation of respiratory rate from pulse oximeters, IEEE Trans. Biomed. Eng. 64 (2017) 1914–1923.
[33] K.H. Shelley, A.A. Awad, R.G. Stout, D.G. Silverman, The use of joint time frequency analysis to quantify the effect of ventilation on the pulse oximeter waveform, J. Clin. Monit. Comput. 20 (2006) 81–87.
[34] L. Nilsson, A. Johansson, S. Kalman, Monitoring of respiratory rate in postoperative care using a new photoplethysmographic technique, J. Clin. Monit. Comput. 16 (2000) 309–315.
[35] P.H. Charlton, Continuous Respiratory Rate Monitoring to Detect Clinical Deteriorations Using Wearable Sensors, Ph.D. Thesis, King's College London, 2017.
[36] C. Orphanidou, Derivation of respiration rate from ambulatory ecg and ppg using ensemble empirical mode decomposition: comparison and fusion, Comput. Biol. Med. 81 (2017) 45–54.
[37] V. Ravichandran, B. Murugesan, V. Balakarthikeyan, K. Ram, S. Preejith, J. Joseph, M. Sivaprakasam, Respnet: a deep learning model for extraction of respiration from photoplethysmogram, in: Proc. 41st Annu. Int. Conf. IEEE Eng. Med. Biol. Soc. (EMBC), IEEE, 2019, pp. 5556–5559.